



Investigating Shrinkage: CAD, Thermal and Volumetric for Selective Laser Sintering of Polyamide Parts

Vishal Sharma¹ · Ramesh Chand² · Vishal S Sharma^{2,3} · Anish Sachdeva² · Sharanjit Singh¹ 

Accepted: 26 November 2020 / Published online: 25 February 2021

© The Author(s), under exclusive licence to Springer Science+Business Media, LLC part of Springer Nature 2021

Abstract

Selective laser sintering (SLS) is an additive manufacturing (AM) process, which is widely used for fabrication of end used products, directly from computer aided design (CAD) data. SLS process is usually used in different areas such as biomedical, automobile and aerospace industries. The major advantage of this process is that the designer can visualize and test the specimens before the full scale production of parts. Therefore, to achieve a good dimensional accuracy in order to fulfill the demands of these fields is a key parameter. Dimensional accuracy of SLS process is mainly influenced by geometry, process parameters and materials. It can only be enhanced by controlling the shrinkage of parts. Therefore, this work is carried out to analyze the effect of crucial contributing factors (i.e, laser power, bed temperature, layer thickness, scan spacing and orientation) for the shrinkage (CAD, thermal and volumetric) of duraform polyamide specimens. Face centered central composite (CCD) design is used for the collection of data. Response surface methodology (RSM) is used to monitor the effects as well as interactions of selected parameters, and for the development of regression models. Multi-response optimization of shrinkage along with composite desirability is employed for different optimized selected SLS parameters. It has been found that the laser power 41 W, bed temperature 170 °C, layer thickness 0.09 mm, scan spacing 0.15 mm and orientation 85.68 degree is a most significant optimized range of these parameters to improve the overall shrinkage measures of parts.

Keywords Process parameters · CAD shrinkage · Thermal shrinkage · Volumetric shrinkage and selective laser sintering

Nomenclature

ANOVA Analysis of variance
AM Additive manufacturing

✉ Sharanjit Singh
malhi.sharanjit@gmail.com

A	Laser power
B	Bed temperature
CCD	Central composite design
CAD	Computer aided design
C	Layer thickness
D	Scan spacing
ED	Energy density
E	Orientation
RSM	Response surface methodology
RP	Rapid prototyping
SLS	Selective laser sintering

Introduction

Rapid Prototyping (RP) includes a number of systems consisting: material jetting, photo polymerization, laminated sheet, binder jetting, directed energy deposition and material extrusion [1]. From all these processes, selective laser sintering (SLS) is one, which is widely used because of extensive range of thermoplastics powders. These powders are such as: polycarbonate, nylons, polyamides and ABS etc. The metal powders like aluminum, titanium, and stainless steel powders are generally used for manufacturing of parts [2]. Fabricated SLS parts are successfully utilized by various industries like aerospace, automotive and medical applications [3]. In SLS process, components are directly created from computer aided design (CAD) data. Initially, STL file is converted into sliced layers, which generates contour information of every layer. Then a layer of powder having desired thickness is uniformly laid over the part bed with the help of roller. In this process powder is not fully melted, but before sintering, bed temperature is raised (because off infrared heaters) to just below the melting point of powder used, to pre heat it. This pre heating of powder particles is required to minimize curling and thermal distortion. This whole process is carried out in nitrogen medium to avoid oxidation. After sintering of top layer, the part bed gets lowered as per required layer thickness and then a fresh layer of powder particles is spread over the part bed [4]. SLS is commonly employed because of its comparatively less trial run cost and SLS consumes less time to present the product in the market [5].

Background

In SLS process, shrinkage is a crucial issue in the performance as well as quality of the products. The material is subjected to significant expansion and contraction during sintering. When tolerating for shrinkage, the amount of changes can be effected by the type of polymer. The polymers are divided into two types: amorphous and semi crystalline. In an amorphous polymer monomers are not arranged in order. But in a semi-crystalline polymer, monomers are arranged in an order and forms a well-defined crystal structure. A semi-crystalline polymers has higher shrinkage than amorphous polymers. This is because when these are cooled down, in a semi crystalline polymers, the macromolecular chains are rearranged to

from well-defined crystallite structure and requires less space for the same number of atoms. Hence the material after the sintering can be expanded or contracted. Improper cooling of frameworks effects in achieving the desired dimensions in specimens, and also results in warpage and shrinkage [6]. When the specimens are removed from the laser bed chamber, these are exposed to new boundary (affecting /environmental) conditions (mechanical and thermal conditions). In SLS process, specimens are built with slight dimensional tolerances. Measurement of these specimens can be influence by the geometry, material and methodology settings [7, 8]. But in case of polymer materials, the shrinkage is a common factor and this is unavoidable. Shrinkage can be a linear, thermal and volumetric. Though the specimens built by SLS process, does not attain the desired shape and size, because of these shrinkages. To control the influence of shrinkage in SLS process, Wang [9] have derived the formula in relation to shrinkage and beam offset. Beam offset is being evaluated along with shrinkage measures of parts produced by SLS processes with different materials. Kumar et al. [10] have observed the influence of parameters on the part quality. It is concluded that the dimensional accuracy is highly influenced by the laser power along with bed temperature and micro-hardness of produced parts is only affected by bed temperature. Wang et al. [11] generated a relationship between SLS parameters and shrinkage for enhancing the dimensional accuracy. Different input parameters considered in this work are: laser power, hatch spacing, bed temperature, layer thickness, scanning speed, interval time and scan mode. Wu et al. [12] examined that effect of SLS parameters (scan count and fill laser power) on morphology and properties of polyamide 12. Scanning electron microscope (SEM) and polarized light microscopy (PLM) micrograph were analyzed to check the obtained results. Further Raghunath et al. [13] have investigated that scan length and laser power are major parameters that effect the shrinkage towards X direction, shrinkage towards Y direction is affected by scan speed and laser power, in Z direction it is influenced by bed temperature, scan speed and scan spacing. Ali et al. [14] have examined that scanning pattern, scan speed, bed temperature, laser power and layer thickness are input factors that effects the shrinkage of parts. Optimization algorithm is developed for investigation of key process parameters for reducing the warpage in parts. Baturynska [15] investigated that dimensional accuracy can be improved by predicting the scaling factors of the part. The result demonstrate that. STL model properties have impact on set of the dimensional features due to orientation. Guo et al. [16] have analyzed the effect of energy input i.e. laser power and surrounding temperature for accuracy, microstructure and mechanical properties of sintered products. Jain et al. [17] found that SLS processed parts are highly influenced by delay time. They purposed an optimization algorithm to develop an optimum factors for increasing the strength of parts. Yeganeh et al. [18] implemented an algorithm in a finite element simulation and optimized process parameters such as: scanning length and offsets keeping other conditions constant. The generated model verifies part accuracy and surface properties, further production time is improved and part warping is reduced up to 35%.

Negi et al. [19] investigated that bed temperature, scan speed and hatch spacing, laser power and scan length have higher impact on the shrinkage behavior of SLS parts. They also predicted shrinkage using artificial neural network (ANN) and presented an

optimization algorithm. Singh et al. [20] investigated the influence of SLS parameters like hatch spacing, laser power, bed temperature, hatch length, and scan count on the shrinkage of parts. It is investigated that the hatch spacing is the highest key factor that influence the shrinkage in generated parts. Yang et al. [21] examined that shrinkage rates are varying with part position in the build chamber. It is noticed that accuracy can be improved by properly adjusting the scale factors. Hireen et al. [22] examined that the accuracy of SLS made parts with the influence of different process parameters using CL50WS Maraging steel (developed by Concept Laser Inc) material. They evaluated that layer thickness is the highest significant parameter that effects the dimensional accuracy of parts.

Senthilkumaran et al. [23] examined the shrinkage behavior of SLS parts with polyamide material for different part orientation and exposure strategies. It is concluded that part orientation effects the shrinkage. Shrinkage is extremely non-uniform in the Y direction and enhanced with the rise in hatch length. Rong-Ji et al. [24] predicted the shrinkage of parts by developing a neural network model in relation to the input factors. The generated neural network model has capability to forecast the part shrinkage prior to the fabrication of parts. Asiabanpour et al. [25] investigated the effect of different SLS parameters using response surface methodology (RSM) on the accuracy of produced parts. Ning et al. [26] examined the influence of scan length on heterogeneity and material anisotropy for direct metal laser sintering (DMLS). It is found that low homogenous parts having higher shrinkage values, which are produced at lower scan length. To control this effect, genetic algorithm is also presented. Shi et al. [27] studied different powder properties, such as particle size, molten viscosity, molecular weight and crystallization rate, for improving the quality of SLS made parts. During this study it is investigated that the part accuracy is highly influenced by crystallization rate. Singh et al. [4] investigated the influence of selected parameters: laser power, hatch length, scan spacing, bed temperature and sinter scan, on the shrinkage of SLS samples using the RSM approach. It is found that scan spacing will act as key factor while controlling the shrinkage of these parts.

In above literature review, it is concluded that the polymer material is already investigated or validated by several past researchers. It is further concluded that shrinkage measures is key concern of the SLS made parts using polymer material. Therefore, in current work, the capability of SLS using polyamide12 (PA12) powder is explored by relating and optimizing parameters for different shrinkage measures. Shrinkage in polymers is majorly influenced by process characteristics, change in temperature and crystallization [27]. Thermal shrinkage is influenced by temperature change when no phase transformation occurs and can be measured by linear expansion. Crystallization may influence the accuracy i.e. change in volume occurs at different cooling rates of polyamide parts. Therefore, the main objective of current study is to examine the influence of selected parameters and to present optimized setting of these parameters for output measures i.e. CAD shrinkage, thermal shrinkage and volumetric shrinkage of specimens using RSM approach. The choice of process parameters requires carefulness because these effects the dimensional accuracy and efficiency of specimens. This investigational plan designed uses the specified settings as per face-center central CCD based on RSM technique. RSM is a set of mathematical as well as statistical approach [8]. This technique is useful for optimization of issues which are influenced by certain variables.

Experimental Details

Below section discusses the experimental as well as methodology details carried out in this work. Flow chart pertaining to experimental procedure is also presented in Fig. 1.

Selection of Parameters

SLS process consist of a set of process parameters as illustrated in Fig. 2. From which laser power (A), bed temperature (B), layer thickness (C), scan spacing (D) and orientation (E) have been analyzed for CAD shrinkage, thermal shrinkage and volumetric shrinkage by fabricating different specimens. Laser power is the power of laser that is generated by laser light on the powder bed. With the use of laser power, the powder is heated near to melting temperature during laser scanning. Bed temperature is a temperature of build chamber and maintained just below the melting temperature of used powder. Layer thickness is the thickness of powder layers to be processed/sintered in single process cycle. Scan spacing is the space among neighboring scan vector, or it is the separation between two consecutive laser beams. Orientation is the arrangement of specimen in build along X, Y and Z direction. The range for laser power and scan

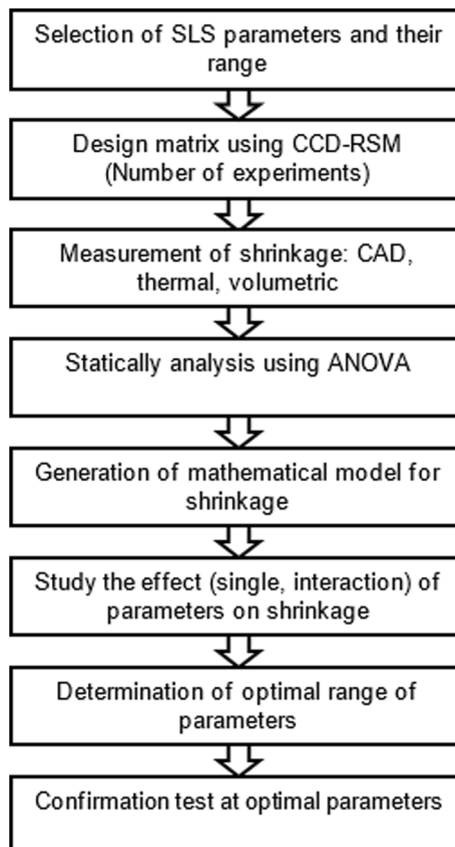


Fig. 1 Flow chart of the experimental sequence followed in this study

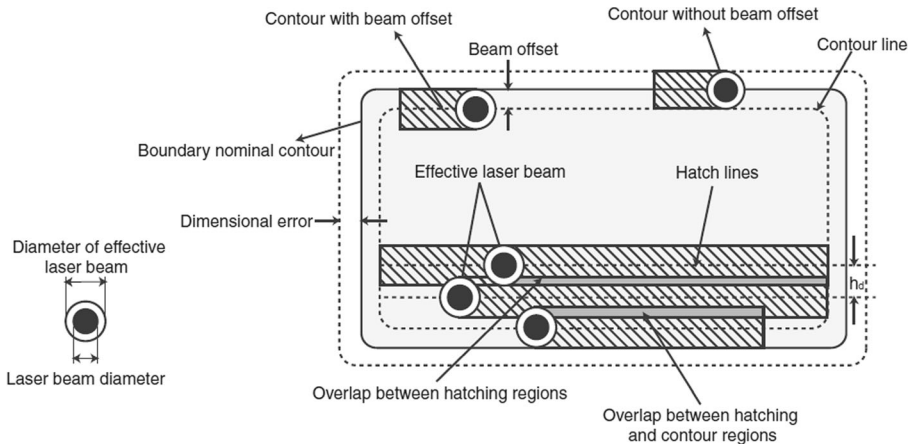


Fig. 2 Different process parameters [28]

spacing is set as per energy density (ED). It is the energy provided to the material per unit area at the surface [23]. When ED increases the fusion of powder particles is higher, and when ED decreases the fusion of powder particles is poor. But in case of SLS, material does not melt fully, it can only be heated up to 80% of melting temperature where material can bind properly and parts are generated. So the range of ED set very carefully to avoid lack of fusion of powder material and degradation. The ED is calculated by equation no. (1) as shown below

$$\text{Energy density}(ED) = \frac{\text{Laser power}}{\text{Scan speed} \times \text{Scan spacing}} \quad (1)$$

Therefore, selection of different working parameters ranges (as illustrated in Table 1), are sorted by an expert opinion and literature review [20].

Detail of Material

The specimens are prepared by using the duraform polyamide material having an average grain size of 60 μm as provided by 3D systems (<https://www.3dsystems.com/materials/>)

Table 1 Process parameters and their values used for experiment

Parameters	Unit	Symbol	Levels			Constant Parameters	
			-1	0	+1		
Laser power	W	A	35	38	41	Roller speed	254 mm/s
Bed temperature	$^{\circ}\text{C}$	B	170	173	176	Sinter scan	ON
Layer thickness	MM	C	0.9	0.1	0.11	Beam Offset	0.25 mm
Scan spacing	MM	D	0.15	0.2	0.25	Spot Size	0.05 mm
Orientation	Deg.	E	0°	45°	90°	Scan Speed	5000 mm/s

duraform-pa)[29]. This material is a linear, semi crystalline in nature. It is a generally reformed with plasticizers and reinforcements of Nylon 12, has minimal moisture absorption with highly stable dimensions in the un-filled nylon materials. This material is used in a progressive engineering areas such as automobile industry (modeling and end use parts-dash board and bumpers etc.), medical fields (artificial body parts) and electronics field (mobile phone body parts and chips etc.). The ratio of material used for fabrication was 70% earlier used powder and 30% unused powder. Higher percentage of recycled powder generates variable quality of laser sintered specimens [29] and higher quantity of fresh powder results curling and warpage [30].

Test Specimens and Performance Measures

The specimens (Fig. 3) having length-120 mm, width-12 mm and thickness-3 mm respectively, are designed for testing with the use of CAD software (Pro-e). CAD model of specimen is transferred in. STL file format. After changing in. STL file further alteration in CAD model design is not possible. This generated. STL file is transferred to machine software (magic software) for orientation and positioning of number of specimens. In this study, three performance measures are taken into account ie CAD shrinkage, thermal shrinkage and volumetric shrinkage.

CAD shrinkage (CS): It is evaluated by measuring of length (L), width (W), Height (H) of each specimen. Every dimension is measured three times and mean of these value is taken as final value. The CAD shrinkage is calculated by equation no. (2) as shown below. All values are measured using digital vernier caliper containing least count of 0.01 mm [31].

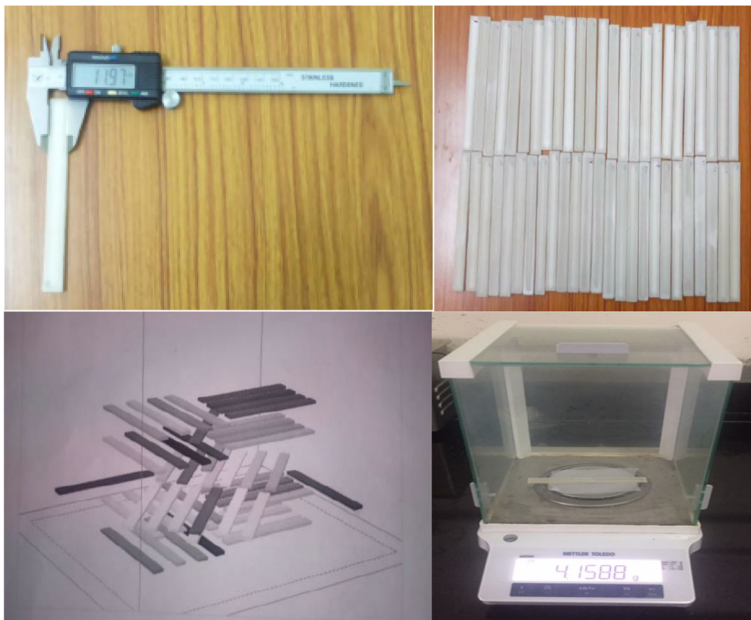


Fig. 3 Dimension measurement of specimen, fabricated specimens in single build, position of specimen in build (orientation X, Y direction only), weight measurement of specimen

$$CS = \left[\frac{(A_1 - A_0)}{A_0} \right] \times 100\% \quad (2)$$

A_0 = design size of cad drawing, A_1 = actual size measured from vernier caliper.

Thermal shrinkage (TS): Normally when heat is added to or removed from a solid material there is a change in temperature (ΔT), and a change in dimensions (ΔL). The relative change in dimensions, or the thermal expansion $\frac{(dl)}{L}$, is usually expressed in a percent. Therefore, the thermal shrinkage is calculated by equation no. (3) as shown below [32].

$$TS = \frac{dl}{l} \quad (3)$$

dl = change in length and l = original length.

Volumetric shrinkage (VS): The volumetric shrinkage is calculated by the difference among the MEASURED volume V_{actual} (measured with digital vernier caliper) and the volume of the generated part. The actual volume of the part is calculated from the mass (m) of the part and taking density (ρ) of the used powder, as provided by 3D systems (<https://www.3dsystems.com/materials/duraform-pa>) (<https://www.3dsystems.com/materials/duraform-pa>)[29]. To calculate volumetric shrinkage expression used is given in Eq. (4) as follow [33]:

$$VS = V_{\text{actual}} - \frac{\text{mass}}{\text{density}} \quad (4)$$

Design of Experiment: Response Surface Methodology

In manufacturing processes, model generation and optimization are two main concerns. RSM is a set of mathematical and a statistical approach. This method is suitable for optimization of issues, which are influenced by set of variables [34]. RSM technique helps to find a focused relationship among output variable (y) and the set of independent input variables. This technique not only improve the efficiency of technologist but also develops part supremacy. The ideal solution has been obtained from regression Eq. 5 and by inspecting response surface contours [35].

$$Y = \beta_0 + \sum_{j=1}^k \beta_j X_j + \sum_{j=1}^k \beta_{ij} X_j^2 + \sum_{i < j=1}^k \beta_{ij} X_i X_j + e_i \quad (5)$$

In above Eq. (5), Y is mainly expected response; β_0 is a constant of coefficient; X_i and Y_j are coded parameters; β_j , β_{ij} and β_{ij} are the interaction coefficients of parameters of linear, second-order and quadratic term; and e_i is random error [35].

In RSM, CCD is the best suited design to analyze functional relation among input parameters and output measures. In CCD each parameter has five level, but when the value of $\alpha = 1$ then the level of every parameter is set as three (max, min and middle level). The total set of experiments can be calculated by $2f + 2f + n$, where f denoted input parameters and n denotes total design points in cube. When comparing with box

behnken design, CCD can also include runs having extreme upper and lower settings (of input factors). Face-center central CCD design is employed in this study because it can fit full quadratic model and best suited in case of sequential experimental plan. While comparing RSM with taguchi technique, in RSM generated models and ANOVA tables are significant factors to analyze the obtained results. From these the significance of each parameter as well as interaction effect among parameters can also be easily determined. Further desirability criteria in RSM also determines optimal conditions from the set of experiments.

A total 50 set of experiments are performed using five input variables, ED (equation no. 1) and three output variables as presented in Table 2.

Result and Discussion

Analysis for CAD Shrinkage

The importance and the significance of different selected process parameters are analyzed with the application of analysis of variance (ANOVA). The 2FI model is employed because the data is best fitted to monitor the CAD shrinkage of SLS parts. A significant model F value (34.71) is obtained due to noise (with chance of 0.01%) and presented in Table 3(a). Lower probability value ($\text{Prob}>F < 0.0500$) depicts a significant model for CAD shrinkage [36]. The terms of model containing values >0.1000 are non-significant. The 4.57 value obtained for lack of fit is significant in relation to pure error. Value of Pred R^2 obtained 0.8047 is in realistic good in relation with the value of Adjusted R^2 , which is 0.8281. The value obtained for adequate precision ratio of generated model is 24.595 (>4), this shows an ample sign for the generated model. The value of PRESS is 80.74, which shows, how the model fits each point in the design.

- Model formulation

The model generated for CAD shrinkage contains B, C, D, E, BD, BE and DE as significant parameters. The nonsignificant parameters, having there partial influence, have been eliminated from the model for its improvement. With use of actual parameters, an empirical relationship developed between output and input parameters, which is expressed in mathematical Eq. 6.

$$CS = -360.77967 + 2.15459 \times B - 67.36111 \times C + 1662.61714 \times D - 0.92822 \times E - 9.80122 \times BD + 5.71984 \times 10^3 \times BE - 0.20754 \times DE \quad (6)$$

Normal probability plots confirms that whether the obtained model or data relates to real system or not. For analyzing the obtained model for CAD shrinkage, normal probability graphs of the studentized residuals and the predicted vs actual graph have been drawn. Figure 4(a) show the normal probability plot for CAD shrinkage. In the obtained graphs, it is observed that the residuals are allined along the straight line for CAD shrinkage. In Fig. 4(b), the predicted data of CAD shrinkage, which are presented using developed model and the experimental data is randomly distributed.

Table 2 Design matrix and collected data

S No	Laser Power (W)	Bed Temp.(°C)	Layer Thickness (mm)	Scan Spacing (mm)	Orientation (deg)	Energy Density (jmm ⁻²)	CAD shrinkage	Thermal shrinkage	Volumetric shrinkage (mm ³)
1	41	176	0.11	0.15	90	0.054666667	5.1875	13.5634	5.00547
2	38	173	0.1	0.25	45	0.0304	-0.84861	13.0305	4.20884
3	35	170	0.11	0.15	90	0.046666667	-1.52083	12.4978	4.10011
4	38	173	0.11	0.2	45	0.038	-4.90139	12.7711	3.69709
5	35	176	0.09	0.15	90	0.046666667	8.5	13.6362	5.49522
6	35	170	0.11	0.25	0	0.028	-2.49167	12.4597	3.99156
7	35	176	0.09	0.25	0	0.028	-3.75694	13.3686	3.84232
8	35	176	0.09	0.15	0	0.046666667	2.175	13.3366	4.58325
9	35	173	0.1	0.2	45	0.035	-1.19306	12.673	4.15519
10	38	173	0.1	0.2	45	0.038	-0.83611	12.7578	4.20579
11	38	173	0.1	0.2	45	0.038	-0.50556	12.7411	4.23694
12	38	173	0.09	0.2	45	0.038	-3.31667	12.9094	3.86484
13	35	176	0.11	0.25	0	0.028	-3.14306	13.1874	3.90958
14	41	170	0.09	0.15	90	0.054666667	-0.1	12.3607	4.2832
15	41	170	0.11	0.25	90	0.0328	-3.05833	12.1604	3.90804
16	38	176	0.1	0.2	45	0.038	-0.51111	13.6271	4.22807
17	38	173	0.1	0.2	45	0.038	0.168056	12.7947	4.33322
18	41	176	0.09	0.25	0	0.0328	-2.69444	13.413	3.94248
19	41	170	0.09	0.25	0	0.0328	-0.44028	12.4487	4.26081
20	38	173	0.1	0.2	45	0.038	-1.73889	12.9195	4.08581
21	35	170	0.09	0.15	90	0.046666667	-0.72639	12.4302	4.19627
22	35	176	0.11	0.15	90	0.046666667	5.77222	13.5541	5.08677
23	41	173	0.1	0.2	45	0.041	-0.53472	13.0825	4.23556
24	35	170	0.11	0.15	0	0.046666667	-2.82083	12.3156	3.95298
25	38	173	0.1	0.2	45	0.038	-0.49028	13.0138	4.23844

Table 2 (continued)

S No	Laser Power (W)	Bed Temp.(°C)	Layer Thickness (mm)	Scan Spacing (mm)	Orientation (deg)	Energy Density (Jmm ⁻²)	CAD shrinkage	Thermal shrinkage	Volumetric shrinkage (mm ³)
26	41	170	0.09	0.25	90	0.0328	-1.86944	12.4855	4.04573
27	35	170	0.09	0.15	0	0.046666667	-0.32222	12.46	4.26642
28	41	176	0.09	0.15	0	0.054666667	4.41111	13.5636	4.88371
29	41	170	0.11	0.15	90	0.054666667	-0.01389	12.8715	4.30092
30	38	173	0.1	0.2	0	0.038	-1.65694	13.0883	4.09911
31	35	176	0.11	0.15	0	0.046666667	0.134722	13.7113	4.32743
32	38	173	0.1	0.2	90	0.038	1.04167	12.6783	4.41091
33	41	176	0.09	0.15	90	0.054666667	8.90694	12.9899	5.57107
34	38	173	0.1	0.2	45	0.038	-0.73333	12.5805	4.20602
35	38	173	0.1	0.2	45	0.038	-0.67917	13.3452	4.21415
36	38	173	0.1	0.15	45	0.050666667	2.71528	12.7191	4.6651
37	35	176	0.09	0.25	90	0.028	-0.57361	14.188	4.22444
38	41	170	0.11	0.15	0	0.054666667	-1.45694	13.5686	4.11435
39	41	176	0.11	0.25	0	0.0328	-3.98056	14.7908	3.80804
40	38	173	0.1	0.2	45	0.038	0.154167	13.0127	4.32489
41	41	170	0.09	0.15	0	0.054666667	-0.3	12.3618	4.26934
42	35	170	0.09	0.25	0	0.028	-2.33611	12.4809	4.00092
43	35	170	0.11	0.25	90	0.028	-2.36528	12.1445	3.9938
44	41	176	0.11	0.25	90	0.0328	-2.16944	13.6567	3.99962
45	41	170	0.11	0.25	0	0.0328	-3.15694	12.0504	3.89478
46	41	176	0.11	0.15	0	0.054666667	2.90833	14.0153	4.68759
47	41	176	0.09	0.25	90	0.0328	-1.45972	14.3189	4.11287
48	35	170	0.09	0.25	90	0.028	-2.22083	13.255	4.03035
49	35	176	0.11	0.25	90	0.028	-1.95	13.3177	4.04674
50	38	170	0.1	0.2	45	0.038	-3.12083	12.2971	3.89746

Table 3 ANOVA and adequacy of 2FI model (a) CAD shrinkage (b) thermal shrinkage (c) volumetric shrinkage

Source	Sum of Squares	DF	MeanSquare	F Value	Prob > F	
(a) CAD Shrinkage						
Model	352.44	7	50.35	34.71	< 0.0001	significant
B	62.45	1	62.45	43.06	< 0.0001	
C	15.43	1	15.43	10.64	0.0022	
D	152.32	1	152.32	105.02	< 0.0001	
E	27.02	1	27.02	18.63	< 0.0001	
BD	69.17	1	69.17	47.69	< 0.0001	
BE	19.08	1	19.08	13.16	0.0008	
DE	6.98	1	6.98	4.81	0.0339	
Residual	60.92	42	1.45			
Lack of Fit	58.36	35	1.67	4.57	0.0215	significant
Pure Error	2.55	7	0.36			
Cor Total	413.35	49				
Std. Dev.		1.2		R-Squared		0.8526
Mean		-0.48		Adj R-Squared		0.8281
C.V.		-251.74		Pred R-Squared		0.8047
PRESS		80.74		Adeq Precision		24.595
(b) Thermal Shrinkage						
Model	14.09	9	1.57	16.21	< 0.0001	significant
A	0.21	1	0.21	2.19	0.1463	
B	11.29	1	11.29	116.84	< 0.0001	
C	0.012	1	0.012	0.12	0.7302	
D	0.019	1	0.019	0.2	0.661	
E	7.71E-03	1	7.71E-03	0.08	0.7791	
AC	0.69	1	0.69	7.15	0.0108	
AE	0.38	1	0.38	3.98	0.0528	
CD	0.83	1	0.83	8.58	0.0056	
CE	0.65	1	0.65	6.74	0.0131	
Residual	3.86	40	0.097			
Lack of Fit	3.48	33	0.11	1.93	0.1859	not significant
Pure Error	0.38	7	0.055			
Cor Total	17.96	49				
Std. Dev		0.31		R-Squared		0.7848
Mean		13.02		Adj R-Squared		0.7364
C.V		2.39		Pred R-Squared		0.6154
PRESS		6.91		Adeq Precision		15.787
(c) Volumetric Shrinkage						
Model	6.39	7	0.91	34.69	< 0.0001	significant
B	1.15	1	1.15	43.65	< 0.0001	
C	0.27	1	0.27	10.39	0.0025	

Table 3 (continued)

Source	Sum of Squares	DF	MeanSquare	F Value	Prob > F	
D	2.69	1	2.69	102.38	< 0.0001	
E	0.47	1	0.47	17.69	0.0001	
BD	1.28	1	1.28	48.62	< 0.0001	
BE	0.37	1	0.37	14.15	0.0005	
DE	0.16	1	0.16	5.98	0.0188	
Residual	1.1	42	0.026			
Lack of Fit	1.06	35	0.03	5.06	0.016	significant
Pure Error	0.042	7	6.00E-03			
Cor Total	7.49	49				
Std. Dev.		0.16		R-Squared		0.8526
Mean		4.25		Adj R-Squared		0.828
C.V.		3.82		Pred R-Squared		0.801
PRESS		1.49		Adeq Precision		24.534

Analysis for Thermal Shrinkage

For thermal shrinkage the 2FI model is used because the data is best fitted to monitor the thermal shrinkage of SLS parts. A significant model F value (16.21) is obtained due to noise (with chance of 0.01%) and presented in Table 3(b). Lower probability value ($\text{Prob}>F < 0.0500$) depicts a significant model for thermal shrinkage [36]. The terms of model containing values >0.1000 are non-significant. The 1.93 value obtained for lack of fit is not significant in relation to pure error. So there is a probability of 18.59% that this large value of lack of fit occurs due to noise which is otherwise desirable. It is good if lack of fit is non-significant. Value of Pred R^2 obtained 0.6154 is in realistic good in relation with the value of Adjusted R^2 , which is 0.7364. The value obtained for adequate precision ratio of generated model is 15.787 (>4), this shows an ample sign for the generated model. The value of PRESS is 6.91, which shows, how the model fits each point in the design.

- Model formulation

The model generated for thermal shrinkage contains B, AC, CD, CE as significant terms. The non significant model terms, having there limited influence, have been eliminated from the model for its improvement. With use of actual parameters, an empirical relationship developed between output and input parameters, which is expressed in mathematical Eq. 7.

$$\begin{aligned}
 TS = & -12.10884 - 0.42698 \times A + 0.19206 \times B - 105.65713 \times C + 32.65684 \times D \\
 & + 0.062226 \times E + 4.89850 \times AC - 8.12235 \times 10^4 \times AE - 321.85813 \\
 & \times CD - 0.31696 \times CE
 \end{aligned} \quad (7)$$

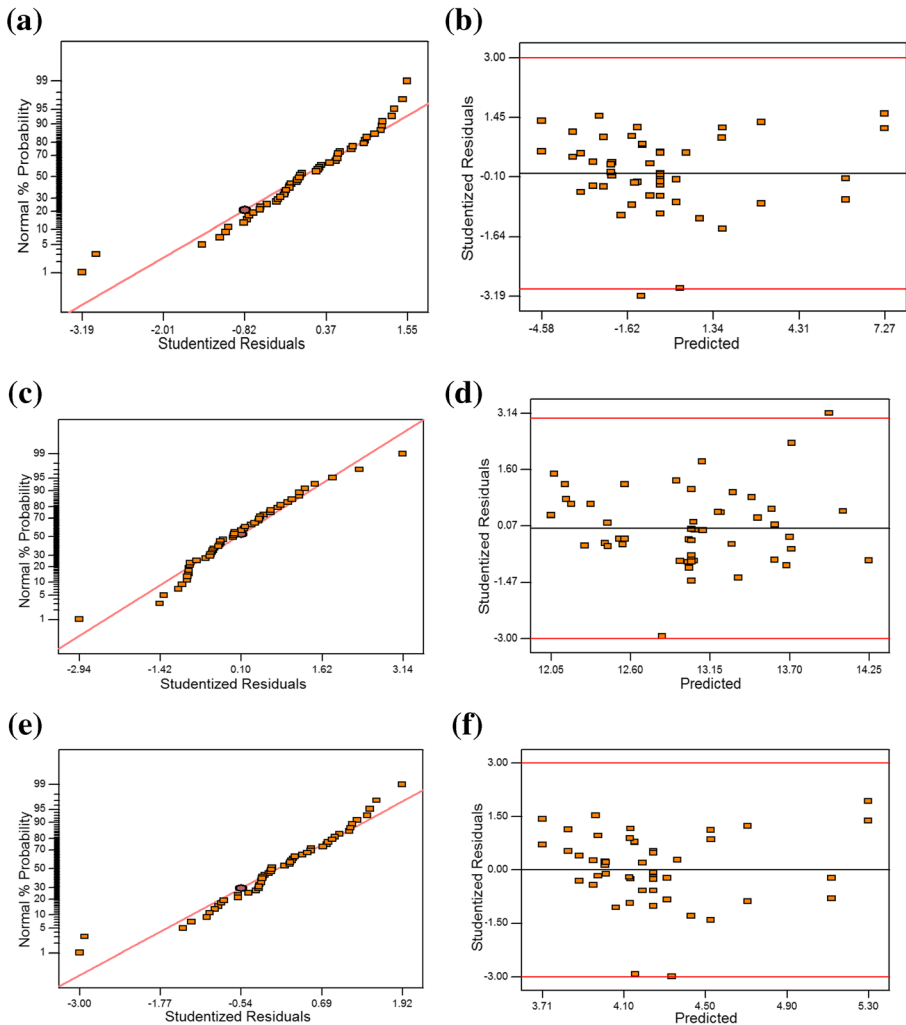


Fig. 4 Normal probability plot of residuals and plot of predicted versus actual response (a, b) CAD shrinkage (c, d) thermal shrinkage (e, f) volumetric shrinkage

Normal probability plots confirms that whether the obtained model or data relates to real system or not. For analyzing the obtained model, normal probability graph of the studentized residuals and the predicted vs actual graph have been drawn. Figure 4(c) shows the normal probability plot for thermal shrinkage. In the obtained graphs, it is observed that the residuals are allined along the straight line for thermal shrinkage. In Fig. 4(d), the predicted values of thermal shrinkage, which are presented using developed model and the experimental data is randomly distributed.

Analysis for Volumetric Shrinkage

For volumetric shrinkage the 2FI model is again used because the data is best fitted to monitor the volumetric shrinkage of SLS parts. A significant model F value (34.69) is

obtained due to noise (with chance of 0.01%) and presented in Table 3(c). Lower probability value ($\text{Prob}>F < 0.0500$) depicts a significant model for volumetric shrinkage [36]. The terms of model containing values >0.1000 are non-significant. The 5.06 value obtained for lack of fit is significant in relation to pure error. Value of $\text{Pred } R^2$ obtained 0.8010 is in realistic good in relation with the value of $\text{Adjusted } R^2$, which is 0.8280. The value obtained for adequate precision ratio of generated model is 24.534 (>4), this shows an ample sign for the generated model. The value of PRESS is 1.49, which shows, how the model fits each point in the design.

- Model formulation

The model generated for volumetric shrinkage contains B, C, D, E, BD, BE, DE as significant parameters. The nonsignificant parameters, having there partial influence, have been eliminated from the model for its improvement. With use of actual parameters, an empirical relationship developed between output and input parameters, which is expressed in mathematical Eq. 8.

$$VS = -44.61477 + 0.29184 \times B - 8.96582 \times C + 226.32471 \times D - 0.12935 \times E - 1.33267 \times BD + 7.98733 \times 10^4 \times BE - 0.031151 \times DE \quad (8)$$

Normal probability plot confirms that whether the obtained model or data relates to real system or not. For analyzing the obtained models, normal probability graph of the studentized residuals and the predicted vs actual graph have been drawn. Figure 4(e) show the normal probability plot for volumetric shrinkage respectively. In the obtained graphs, it is observed that the residuals are allined along the straight line for volumetric shrinkage. In Fig. 4(f), which are presented using developed model and the experimental data is randomly distributed.

Effect of Process Parameters for: CAD Shrinkage, Thermal Shrinkage, Volumetric Shrinkage

- Laser power: The influence of laser power is only observed in case of thermal shrinkage and illustrated in Fig. 5(a). During the analysis of the influence of laser power it can be grasped that thermal shrinkage increases with the increase in the value of laser power from lower level to top level. This is because of when the laser power increases, heat conduction rate also increases, which results in closely packing of powder material. Increase in laser power also transfer high energy to the powder particles which effects in sintering of a material, which enhances the shrinkage. Similar trend is also observed by the Singh et al. [4, 20] during analysis of shrinkage using polyamide powder.
- Bed temperature: Fig. 5 (a, b, c) displays that shrinkage enhances with the increase in the bed temperature. It is observed from the fact that in laser sintering rate of crystallization confirms the tendency of material to curl and probability to achieve desired accuracy. With decrease in temperature the crystallization of material decreases, but at higher temperature because of low cooling rate the molecules get arranged properly. Therefore enhanced packing of powder particles results

higher shrinkage in parts. Singh et al. [4, 20] and Nagi and Sharma [19] also presented that the shrinkage is enhanced at higher temperature.

- Layer thickness: Fig. 5 (a, c) presents that the layer thickness influences the CAD shrinkage as well as volumetric shrinkage. With the enhancement in layer thickness from lower level (0.09 mm) to extreme level (0.11 mm) there is decrease in the CAD shrinkage as well as volumetric shrinkage. The reason behind is that, with the

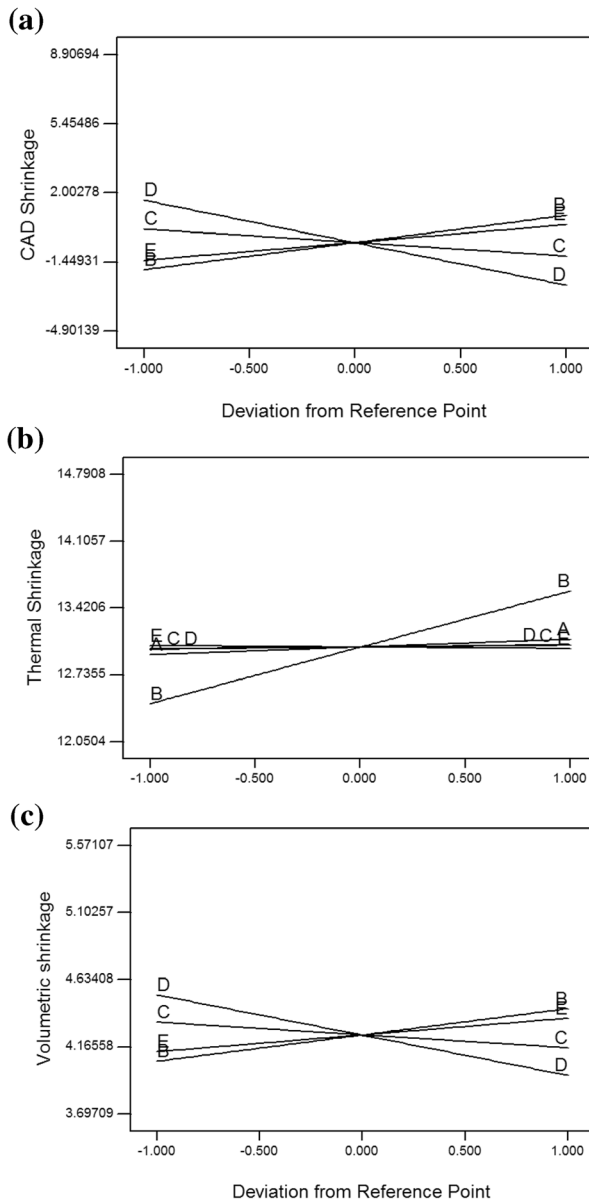


Fig. 5 Influence of various parameters on shrinkage (a) CAD shrinkage (b) thermal shrinkage (c) volumetric shrinkage

increase in layer thickness the thickness of powder layer laid in build also increase, this will affect the in depth melting of powder layer. This will affect the sintering of part and results in lower shrinkage in the obtained parts. But a minute increase is observed in case of thermal shrinkage at higher level of layer thickness when we are analyzing it with layer thickness as shown in Fig. 5(b).

- Scan spacing: In Fig. 5 (a, b, c), a significant effect on CAD shrinkage, thermal shrinkage and volumetric shrinkage have been observed for scan spacing. CAD shrinkage and volumetric shrinkage of parts decreases with the increase in scan spacing from low level (0.15 mm) to higher level (0.25 mm). It occurs because of overlapping of sintered zone at lower scan spacing, which also results repeated heating and cooling sequences in the build. But at higher scan spacing powder particles are not proper packed and the value of scan spacing should always be remain below the laser beam diameter. The high value of san spacing can also cause the curling of fresh layer that may clings to the roller as well. Singh et al. [4, 20] also obtained the similar trend for shrinkage measures the increase in scan spacing. But again minute increase is observed in case of thermal shrinkage as shown in Fig. 5(b) with the increase in scan spacing this trend of shrinkage matches with the observation found by Nagi and Sharma [19].
- Orientation: Fig. 5 (a, b, c) indicates that orientation has significant effect on CAD shrinkage, thermal shrinkage and volumetric shrinkage. It is seen that when orientation increases from 0^0 to 90^0 the CAD shrinkage and volumetric shrinkage also increase. This observation attributes that at the 90^0 orientation, parts have greater width values, so it is difficult to achieve the desired width value and parts are also shrinking during cooling. This whole phenomena leads towards higher shrinkage. This trend get reversed in case of thermal shrinkage as shown in Fig. 5(b).

Interaction Effect of Process Parameters for: CAD Shrinkage, Thermal Shrinkage, Volumetric Shrinkage

- CAD Shrinkage-

Interaction as well as 3D surface plots displays the combined influence of two parameters on the performance measures. Figure 6(a) presents the interaction and surface plot of bed temperature and scan spacing for CAD shrinkage. It has been seen that with the rise in bed temperature form lower level to higher level the CAD shrinkage decreases and further with the rise in the level of scan spacing, CAD shrinkage also increases. Figure 6(b) exhibits the interaction and 3D surface plot between bed temperature and orientation. CAD shrinkage in interaction to both bed temperature as well as orientation increases as the level of these parameters rises from low level to higher level. The interaction graph and 3D plot between scan spacing and orientation for CAD shrinkage has been shown in Fig. 6(c). Diagrams perceived that the increase in the level of orientation and scan spacing from low level to high level, the CAD shrinkage decreases gradually.

- Thermal shrinkage-

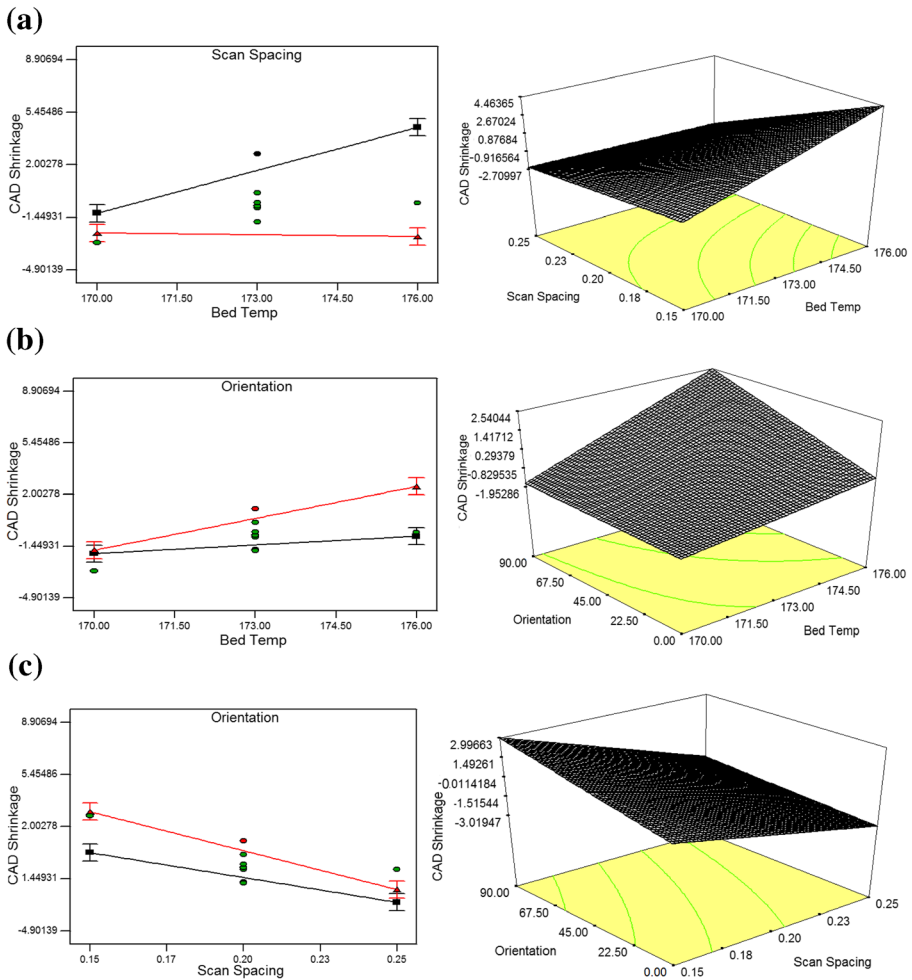


Fig. 6 Interaction graph of parameters for CAD shrinkage (a) scan spacing and bed temp. (b) bed temp. and orientation (c) scan spacing and orientation

In Fig. 7(a) demonstrates the interaction and 3D surface plot among the laser power and layer thickness. The specimen sintered with the level of laser power increasing from 38 W to 41 W the thermal shrinkage in these specimens also increase but with the rise in layer thickness from low level to higher level, the thermal shrinkage decreases. Figure 7(b) show the interaction graph and 3D surface plot between laser power and orientation. It is perceived that the thermal shrinkage increase with the increase in laser power and remains stable with increasing the level of orientation. Figure 7(c) show the interaction graph and 3D surface plot between layer thickness and scan spacing. It can be perceived that as the level of layer thickness increase toward higher side the thermal shrinkage also increase and further thermal shrinkage decrease with increase in the level of scan spacing from lower level to higher level. Figure 7(d) show the interaction and 3D surface plot between layer thickness

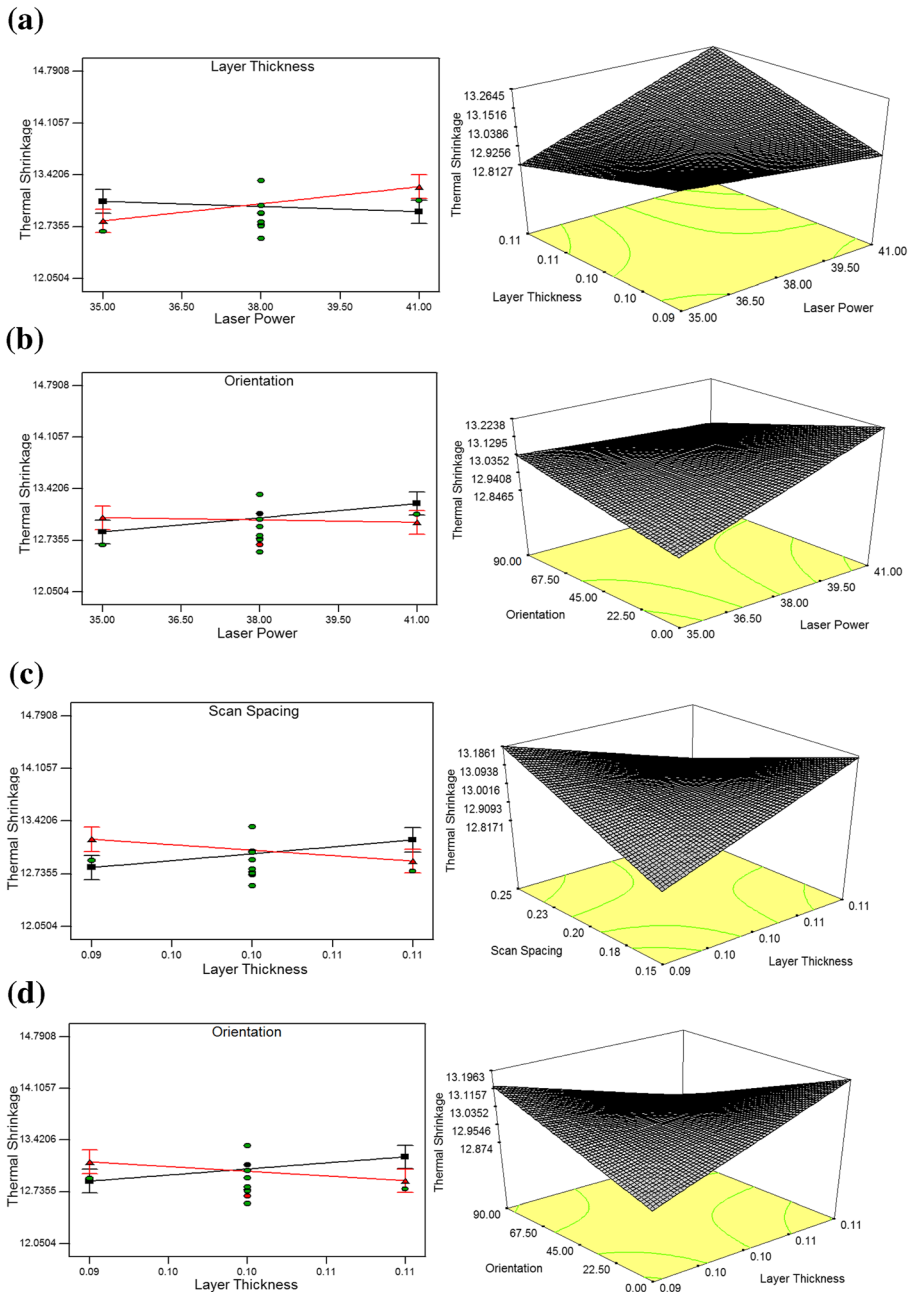


Fig. 7 Interaction graph of parameters for thermal shrinkage **(a)** laser power and layer thickness **(b)** laser power and orientation **(c)** scan spacing and layer thickness **(d)** layer thickness and orientation

and orientation. It can be observed that the thermal shrinkage increases with increasing the level of level of layer thickness and the thermal shrinkage gradually decreases with increasing the level of orientation.

- Volumetric shrinkage-

Figure 8(a) show the interaction and 3D surface plot of layer thickness and orientation versus volumetric shrinkage. With the increase in scan spacing, high volumetric shrinkage is obtained. But as the bed temp increases there is minor decrease in volumetric shrinkage is observed. Figure 8(b) show the interaction and 3D surface plot of bed temp and orientation for volumetric shrinkage. It can be observed that volumetric shrinkage increases with the increase in the level of both bed temperature as well as orientation. Figure 8(c) shows the interaction graph and 3D surface plot of scan spacing and orientation. It has been observed that the volumetric shrinkage decreases with the increase in the level of scan spacing as well as orientation.

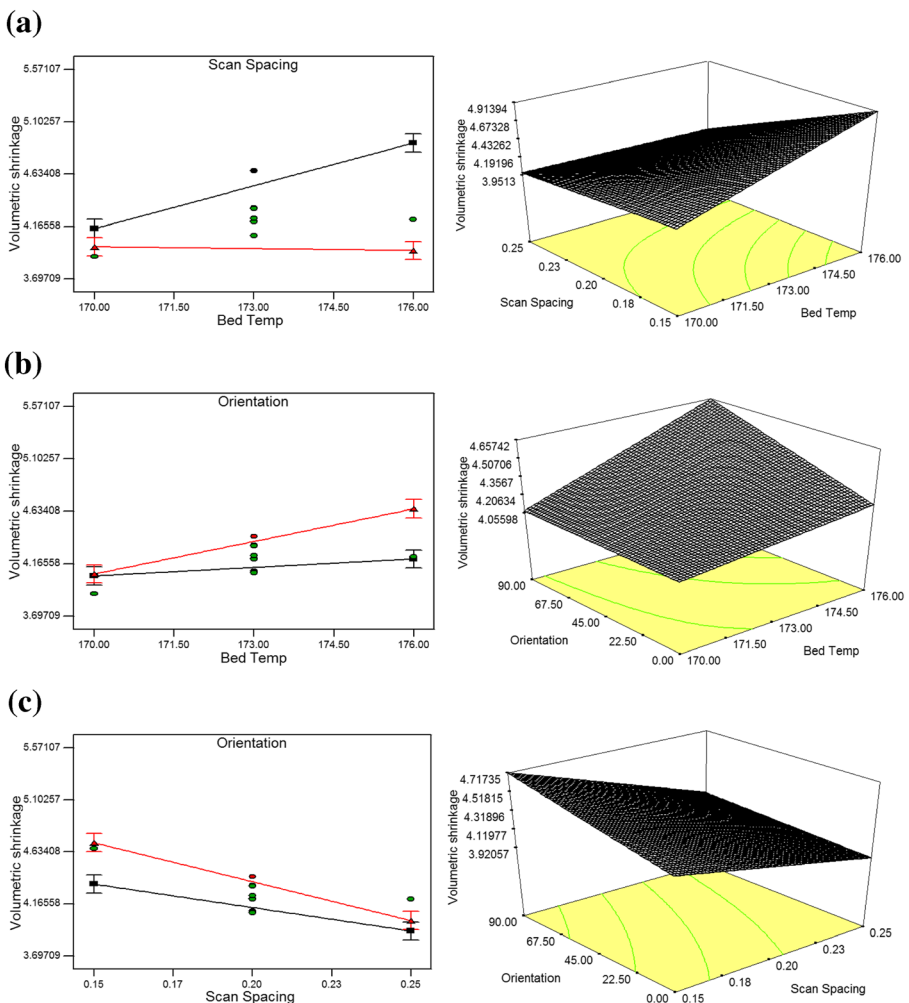


Fig. 8 Interaction graph of parameters for volumetric shrinkage (a) bed temp and scan spacing (b) bed temp and orientation (c) scan spacing and orientation

Optimization

Analysis of Desirability Function

Multi-response optimization is most prominent technique to select desirable condition that fulfil all goal required by desirability function approach. This concept of desirability deals best in case of multi-response optimization. As the desirability value increases the product quality also enhances. In this study optimized set of parameters are obtained keeping CAD shrinkage =0 and thermal shrinkage and volumetric shrinkage at minimum level combined equally. Consequently, a set of objectives is implemented to optimize the generated model in which the optimization value consist of the selected input parameters and obtained responses. All input parameters are selected in range and the goal for output ie CAD shrinkage =0, thermal shrinkage and volumetric shrinkage is to minimize respectively as shown in Table 4(a).

The set of optimal combinations of selected parameters are shown in Table 4(b). The combination that present desirability equals to 86.1% are the optimum combinations, and generated better yield. The shrinkage predicted as per the model using obtained conditions (laser power-41 W, bed temperature – 170 °C, layer thickness-0.09 mm, scan spacing-0.15 mm and orientation-85.68). The value of desirability function is 0.86 obtained for these conditions. The confirmation test are performed to confirm the obtained optimum value. The value of CAD shrinkage –0.01, thermal shrinkage 12.2 and volumetric shrinkage 4.27 is respectively obtained from confirmation tests, these obtained results agrees fine with the predicted values.

Conclusion

In this experimental work, in order to enhance the quality of SLS made parts, the multi-objective optimization of CAD shrinkage, thermal shrinkage and volumetric shrinkage is carried out to analyze the influence of selected parameters on shrinkage of parts. With the application of RSM methodology, all parameters are analyzed with three level. The statistical approach is applied for investigation of different experimental outcomes. The results shows that the R^2 value of the CAD shrinkage, thermal shrinkage and volumetric shrinkage are 85.2%, 78.4% and 85.0% and the AP value are 24.5, 15.7 and 24.53 respectively. This indicates that the fitting of model is good. Further 2FI models are used for the development of all regression models of CAD shrinkage, thermal shrinkage and volumetric shrinkage. Then composite desirability method is employed for multi-objective optimization of performance measures. As the goal for CAD shrinkage =0 and for thermal shrinkage and volumetric shrinkage is set to minimum the optimized combination of selected parameters are: laser power-41 W, bed temperature – 170 °C, layer thickness-0.09 mm, scan spacing-0.15 mm, and orientation-85.68°. The optimal value of CAD shrinkage –0.0100825, thermal shrinkage - 12.19, and volumetric shrinkage –4.30 are obtained with the combined desirability of 86.2%. This shows that the predicted values are in good agreement to the experimental results obtained.

Further it is noticed that the bed temperature, layer thickness, scan spacing and orientation are the significant parameters and influence the all three type of shrinkage

Table 4 (a) RSM optimization range for process parameters and responses (b) Optimization results for process parameters and responses

(a)		Upper	Lower	Upper	Weight	Importance			
Lower	Upper	Goal	Limit	Limit	Weight	Importance			
Name	Goal								
Laser Power	is in range		35	41	1	3			
Bed Temp	is in range		170	176	1	3			
Layer Thickness	is in range		0.09	0.11	1	3			
Scan spacing	is in range		0.15	0.25	1	3			
Orientation	is in range		0	90	1	3			
CAD shrinkage	is target = 0		-4.90139	8.90694	1	3			
Thermal shrinkage	minimize		12.0504	14.7908	1	3			
Volumetric shrinkage	minimize		3.69709	5.57107	1	3			
(b)									
S No.	Laser Power	Bed Temp	Layer Thickness	Scan spacing	Orientation	CAD shrinkage	Thermal shrinkage	Volumetric shrinkage	Desirability
1	41	170	0.09	0.15	85.68	-0.0100825	12.1939	4.30433	0.861
2	41	170.03	0.09	0.15	73.31	-0.107201	12.1908	4.29126	0.859
3	41	170.37	0.09	0.15	56.41	-9.18E-06	12.2504	4.30607	0.855
4	36.66	170.96	0.09	0.15	23.79	-0.00123299	12.3728	4.30559	0.841
5	35.47	171.04	0.09	0.15	13.48	-0.128394	12.3448	4.28813	0.841
6	37.22	171.03	0.09	0.15	13.62	-0.13731	12.3475	4.28693	0.841
7	35.08	170.55	0.1	0.15	90	-0.00627238	12.5306	4.30736	0.822
8	39.11	170	0.09	0.18	0	-1.2091	12.2413	4.15011	0.81
9	35.09	170	0.1	0.17	0	-1.54016	12.206	4.10271	0.797
10	35.27	173.03	0.1	0.15	0	1.85E-06	12.9283	4.30601	0.771

measures. Laser power have only influence on the thermal shrinkage. The thermal shrinkage increases with the increase in laser power from low level to higher level. Bed temperature has same influence in all type of shrinkage measures i.e. with the increase in bed temperature all three: CAD shrinkage, thermal shrinkage and volumetric shrinkage increases gradually. With the increase in scan spacing the CAD shrinkage and volumetric shrinkage decreases gradually but there is minute increase in case of thermal shrinkage. During interaction of CAD shrinkage and volumetric shrinkage with orientation, both of these increases with the increase in the orientation but in case of thermal shrinkage this trend get reversed.

References

1. Chua, C.K., Leong, K.F., Lim, C.S.: Rapid prototyping: principles and applications. 3rd Ed., World Scientific; Singapore (2010)
2. Klocke, F., Arntz, K., Teli, M., Winands, K., Wegener, M., Oliari, S.: State-of-the-art laser additive manufacturing for hot work tool steels. *Procedia CIRP*. **63**, 58–63 (2017)
3. Shah, K., Pinkerton, A.J., Salman, A., Li, L.: Effects of melt pool variables and process parameters in laser direct metal deposition of aerospace alloys. *Mater Manuf Process*. **25**(12), 1372–1380 (2010)
4. Singh, S., Sharma, V.S., Sachdeva, A.: Optimization & analysis of shrinkage in selective laser sintered polyamide parts. *Mater Manuf Process*. **27**(6), 707–714 (2012)
5. Singh, S., Sharma, V.S., Sachdeva, A.: Progress in selective laser sintering using metallic powders: a review. *Mater Sci Technol*. **32**(8), 760–772 (2016)
6. Manoraj, M., Ansari, M.N.M., Shakes, R.A.: Review on the effects of process parameters on strength, shrinkage, and warpage of injection molding plastic component. *Polym Plast Technol Eng*. **56**, 1–12 (2017)
7. Avraam, I.: Injection and compression molding fundamentals. Marcel Dekker Inc, New York (1987)
8. Aldahdooh, M., Bunnori, N.M., Johari, M.: Evaluation of ultra-high performance fibre reinforced concrete binder content using the response surface method. *Mater Des*. **52**, 957–965 (2013)
9. Wang, X.: Calibration of shrinkage and beam offset in SLS. *Rapid Prototyp J*. **5**(3), 129–133 (1999)
10. Kumar, N., Kumar, H., Khurmi, J.S.: Experimental investigation of process parameters for rapid prototyping technique (selective laser sintering) to enhance the part quality of prototype by Taguchi method. *Procedia Technol*. **23**, 352–360 (2016)
11. Wang, R.J., Wang, L., Zhao, L., Liu, Z.: Influence of process parameters on part shrinkage in SLS: *Int. J. Adv. Manuf. Technol*. **33**, 498–504 (2006)
12. Wu, J., Xu, X., Zhao, Z., Wang, M., Zhang, J.: Study in performance and morphology of polyamide 12 produced by selective laser sintering technology. *Rapid. Prototyp. J*. 1355–2546 (2017)
13. Raghunath, N., Pandey, P.M.: Improving accuracy through shrinkage modelling by using Taguchi method in selective laser sintering. *Int J Mach Tools Manuf*. **47**(6), 985–995 (2007)
14. Dastjerdi, A.A., Movahhedy, M.R., Akbari, J.: Optimization of process parameters for reducing warpage in selected laser sintering of polymer parts. *Addit Manuf*. **18**, 285–294 (2017)
15. Baturynska, I.: Statistical analysis of dimensional accuracy in additive manufacturing considering STL model properties. *Int J Adv Manuf Technol*. **97**(5–8), 2835–2849 (2018)
16. Jiang, G., Jiaming, B., Kui, L., Jun, W.: Surface quality improvement of selective laser sintered polyamide 12 by precision grinding and magnetic field-assisted finishing. *Mater Des*. **138**, 39–45 (2017)
17. Jain, P.K., Pandey, P.M., Rao, P.V.M.: Effect of delay time on part strength in selective laser sintering. *Int J Adv Manuf Technol*. **43**(1–2), 117–126 (2009)
18. Yeganeh, A.M., Movahhedy, M.R., Khodaygan, S.: An efficient scanning algorithm for improving accuracy based on minimizing part warping in selected laser sintering process. *Virtual Phys Prototyp*. **14**(1), 59–78 (2019)
19. Negi, S., Sharma, R.K.: Study on shrinkage behavior of laser sintered PA 3200GF specimens using RSM and ANN. *Rapid Prototyp J*. **22**(4), 645–659 (2016)
20. Singh, S., Sharma, V.S., Sachdeva, A.: Application of response surface methodology to analyze the effect of selective laser sintering parameters on dimensional accuracy. *P. Addit. Manuf*. **4**(1), 3–12 (2019)

21. Yang, H.J., Hwang, P.J., Lee, S.H.: A study on shrinkage compensation of the SLS process by using the Taguchi method. *Int J Mach Tools Manuf.* **42**(11), 1203–1212 (2002)
22. Hiren, M., Gajera, M.E., Dav, K.G., Jani, V.: Experimental investigation and analysis of dimensional accuracy of laser-based powder bed fusion made specimen by application of response surface methodology. *P Addit Manuf.* **4**(4), 371–382 (2019)
23. Senthilkumaran, K., Pandey, P.M., Rao, P.V.M.: Influence of building strategies on the accuracy of parts in selective laser sintering. *Mater Des.* **30**(8), 2946–2954 (2009)
24. Rong-Ji, W., Xin-hua, L., Qing-ding, W., Lingling, W.: Optimizing process parameters for selective laser sintering based on neural network and genetic algorithm. *Int J Adv Manuf Technol.* **42**(11), 1035–1042 (2009)
25. Asiabanpour, B., Palmer, K., Khoshnevis, B.: An experimental study of surface quality and dimensional accuracy for selective inhibition of sintering. *Rapid Prototyp J.* **10**(3), 181–192 (2004)
26. Ning, Y., Song, Y.S., Fuh, J.Y.H.: Effect and control of hatch length on material properties in the direct metal laser sintering process. *J Eng Manuf.* **219**(1), 15–25 (2005)
27. Shi, Y., Li, Z., Sun, H., Huang, S., Zeng, F.: Effect of the properties of the polymer materials on the quality of selective laser sintering parts. *J Mater Des A.* **218**(3), 247–252 (2004)
28. Calignano, F., Manfredi, D., Ambrosio, E.P., Iuliano, L., Fino, P.: Influence of process parameters on surface roughness of aluminum parts produced by DMLS. *Int. J. Adv. Manuf. Technol.* **67**(9–12), 2743–2751 (2012)
29. Dotchev, K., Yusoff, W.: Recycling of polyamide 12 based powders in the laser sintering process. *Rapid Prototyp J.* **15**(3), 192–203 (2009)
30. Dotchev, K., Yusoff, W.: Recycling of polyamide 12 based powders in the laser sintering process. *Rapid Prototyp J.* **15**(3), 192–203 (2009)
31. Chunze, Y., Yusheng, S., Jingsong, Y., Jinhui, L.: Preparation and selective laser sintering of nylon-12 coated metal powders and post processing. *J Mater Process Tech.* **209**, 5785–5792 (2009)
32. Cezairliyan, A., Maglic, K.D., Peletsky, V.E.: (eds.) *Compendium of thermophysical property measurement methods.* Springer Science Business Media New York. (1992)
33. Mukras, S.M.S., Omar, H.M., Al-Mufadi, F.A.: Experimental-based multi-objective optimization of injection molding process parameters. *Arab J Sci Eng.* **44**(9), 7653–7665 (2019)
34. Sharma, V.S., Singh, S., Sachdeva, A., Kumar, P.: Influence of sintering parameters on dynamic mechanical properties of selective laser sintered parts. *Int J Mater Form.* **8**, 157–166 (2015)
35. Montgomery, D.C.: *Design and analysis of experiments.* Wiley, Hoboken (2013)
36. Myers, R.H., Montgomery, D.C., Anderson, C.M.: *Response surface methodology: process and product optimization using designed experiments*, 3rd edn. John Wiley & Sons, New York (2008)

Publisher's Note Springer Nature remains neutral with regard to jurisdictional claims in published maps and institutional affiliations.

Affiliations

Vishal Sharma¹ · Ramesh Chand² · Vishal S Sharma^{2,3} · Anish Sachdeva² · Sharanjit Singh¹

¹ Department of Mechanical Engineering, DAV University Jalandhar, Jalandhar, Punjab 144012, India

² Department of Industrial and Production Engineering, Dr B R Ambedkar National Institute of Technology Jalandhar, Jalandhar, Punjab 144011, India

³ School of Mechanical, Industrial & Aeronautical Engineering, University of the Witwatersrand, Johannesburg, South Africa